

# One-dimensional hydrodynamics of ultrarelativistic heavy-ion collisions

M. -C. Chu

*W. K. Kellogg Radiation Laboratory, California Institute of Technology, Pasadena, California 91125*

(Received 5 May 1986)

We present one-dimensional, relativistic, viscid hydrodynamic calculations for central collisions of  $^{238}\text{U}$  ions at center-of-mass energies up to 100 GeV/nucleon. We find that while the hydrodynamic evolution is very sensitive to the formation and thermalization time and to the models of the source terms, the effects of changing the viscosity and the equation of state are small.

## I. INTRODUCTION

The possibility of creating a quark-gluon plasma in the laboratory has aroused much interest in high-energy heavy-ion collisions.<sup>1</sup> An important ingredient in a theory of ultrarelativistic heavy-ion collisions is the understanding of the dynamics of the process, and hydrodynamics serves as both a plausible and a convenient framework for such a description.

Many authors have considered different aspects of the hydrodynamics of high-energy heavy-ion collisions.<sup>2-8</sup> Most of these calculations adopt a scaling picture<sup>2</sup> for the longitudinal expansion of the energetic volume produced in the collisions, which allows a simple analytic solution. However, Ref. 7 shows that while a one-dimensional approximation is not bad, finite-size effects may significantly modify the scaling behavior of quark-gluon plasma. Kajantie and co-workers,<sup>3</sup> on the other hand, showed that a consistent treatment of the source terms is a necessary refinement of earlier estimates of the initial conditions. Moreover, recent studies suggest that nuclei seem to be not as transparent as they were once thought.<sup>9</sup> This may indicate deviations from the inside-outside cascade model,<sup>10</sup> which was used by most of the hydrodynamic calculations. It is also important to investigate the sensitivity of the hydrodynamics to viscosity, the equation of state, and the formation and thermalization time  $\tau_0$  of the plasma, not only because these parameters are essential ingredients in a study of the properties of quark-gluon plasma, but also because the very existence of the plasma in heavy-ion collisions may depend on the actual values of these parameters.

In this paper we present a one-dimensional, viscid, relativistic hydrodynamic model of high-energy heavy-ion collisions. Our purpose is twofold: we want to make what we believe to be necessary modifications to the earlier calculations, and to probe the importance of several other uncertain parameters. This paper is organized as follows. In Sec. II we derive the hydrodynamic equations. The source terms are then derived in Sec. III from two "benchmark" models: the inside-outside cascade and the multiple collision model. Section IV presents the method of solution and the results. Implications from this work are then discussed in Sec. V, which concludes the paper.

## II. HYDRODYNAMIC EQUATIONS

We start with the stress-energy tensor,  $T^{\mu\nu} = T_0^{\mu\nu} + T_d^{\mu\nu}$ , where

$$T_0^{\mu\nu} = (\epsilon + P)u^\mu u^\nu + Pg^{\mu\nu} \quad (1a)$$

is the ideal part and

$$T_d^{\mu\nu} = -\eta(\partial^\mu u^\nu + \partial^\nu u^\mu + u^\mu u^\alpha \partial_\alpha u^\nu + u^\nu u^\alpha \partial_\alpha u^\mu) - (\xi - \frac{2}{3}\eta)(g^{\mu\nu} + u^\mu u^\nu)\partial_\rho u^\rho \quad (1b)$$

is the dissipative part.<sup>11</sup> Here,  $\epsilon$  and  $P$  are the local energy density and pressure, respectively, and  $u^\mu$  is the four-velocity  $(\gamma, \gamma\mathbf{v})$ . We use the metric  $g^{\mu\nu} = \text{diag}(-1, 1, 1, 1)$ . In writing down Eqs. (1), we follow the Landau-Lifshitz definition and retain only terms of first order in gradients.  $\eta$  and  $\xi$  are the shear and bulk viscosity coefficients.

We also consider the net-baryon-number current:

$$J_B^\mu = n_B u^\mu + v^\mu,$$

where  $n_B$  is the proper net-baryon-number density and  $v^\mu$  is the heat-transport term. In a plasma with zero baryon chemical potential,  $v^\mu$  vanishes because it involves transport of heat with respect to the baryons.<sup>12,13</sup> In the bulk of a quark-gluon plasma created in heavy-ion collisions at energies considered here, the baryon chemical potential and the net baryon density are both small; therefore it is safe to ignore  $v^\mu$ . After all the heat transport term represents a small correction to the baryon-number current which we shall treat approximately only (by considering equations of state not depending on the baryon chemical potential).

We shall consider a central collision along the  $z$  axis in the center-of-mass frame with time  $t$  ( $t=0$  when the first collisions occur). We will also restrict our calculations to collisions of identical nuclei, so that the system is symmetric with respect to the  $z=0$  plane [see Fig. 1(a)]. Hydrodynamic equations can be derived from energy-momentum conservation,  $\partial_\mu T^{\mu\nu} = \Sigma^\nu$ , and net-baryon-number conservation,  $\partial_\mu J_B^\mu = \sigma_B$ , with  $\Sigma^\nu$  and  $\sigma_B$  source terms that describe how energy momentum and net baryon number are created in heavy-ion collisions.<sup>3</sup> In the following we shall ignore the transverse degree of freedom

and only consider the longitudinal ( $z$ ) flow of the plasma. A natural choice of coordinates for one-dimensional relativistic hydrodynamics is  $(\mathbf{e}_s, \mathbf{e}_y)$ , where  $\mathbf{e}_s$  and  $\mathbf{e}_y$  are the unit vectors along the  $s \equiv \ln(\tau/\tau_0)$ ,  $\tau \equiv (t^2 - z^2)^{1/2}$  being the proper time, and

$$y \equiv \frac{1}{2} \ln \left[ \frac{t+z}{t-z} \right]$$

axes. But we shall use a new set of coordinates  $\hat{\mathbf{u}}, \hat{\mathbf{v}}$  defined as

$$\begin{aligned} \hat{\mathbf{u}} &\equiv \frac{1}{a} (\alpha \mathbf{e}_s + \beta \mathbf{e}_y), \\ \hat{\mathbf{v}} &\equiv \frac{1}{a} (\beta \mathbf{e}_s + \alpha \mathbf{e}_y), \end{aligned} \quad (2)$$

in terms of which the hydrodynamic equations are simplified. Here  $\alpha \equiv \sinh(\theta - y)$ ,  $\beta \equiv \cosh(\theta - y)$ ,  $\theta = \text{arccosh} \gamma$  being the local fluid rapidity, and  $a \equiv (\alpha^2 + \beta^2)^{1/2}$ . The set of curves along the  $\hat{\mathbf{u}}$  and  $\hat{\mathbf{v}}$  directions are similar to the characteristics of the flow, except that we use the fluid velocity as seen from a scaling frame,  $\tanh(\theta - y)$ , instead of the velocity of signal propagation.<sup>3,14</sup> Note that if scaling holds,  $\theta = y$ , then the  $\hat{\mathbf{u}}$  and  $\hat{\mathbf{v}}$  axes coincide with the  $y, s$  axes. The directional derivatives along  $\hat{\mathbf{u}}$  and  $\hat{\mathbf{v}}$  are

$$\partial_u = \frac{1}{a} (\alpha \partial_s + \beta \partial_y)$$

and

$$\partial_v = \frac{1}{a} (\beta \partial_s + \alpha \partial_y).$$

The hydrodynamic equations thus obtained are

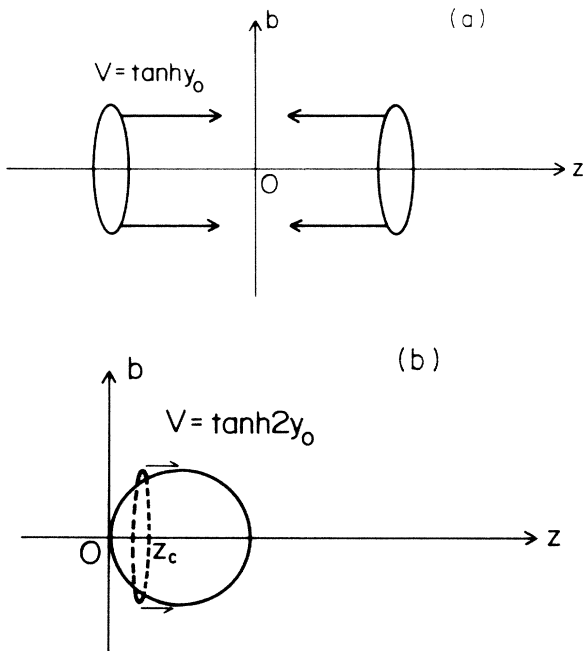


FIG. 1. Central collision of two identical heavy ions in (a) the center-of-mass frame, (b) the target's rest frame.

$$\partial_v \epsilon + (\epsilon + P) \partial_u \theta = \frac{1}{t_d} \chi (\partial_u \theta)^2 + t_d S_1, \quad (3a)$$

$$\begin{aligned} \partial_u P + (\epsilon + P) \partial_v \theta = \frac{1}{t_d} \left\{ \chi \left[ \frac{2\alpha\beta}{a^2} \partial_u \theta + \partial_v \theta \right. \right. \\ \left. \left. - \frac{\alpha}{a} \left[ 2 \frac{\beta^2}{a^2} + 1 \right] \right] \partial_u \theta \right. \\ \left. + \chi \partial_u^2 \theta + \partial_u \chi \right\} + t_d S_2, \quad (3b) \end{aligned}$$

with  $S_1 = \Sigma^0 \cosh \theta - \Sigma^1 \sinh \theta$ ,  $S_2 = \Sigma^1 \cosh \theta - \Sigma^0 \sinh \theta$ , and

$$\partial_v n_B + n_B \partial_u \theta = t_d \sigma_B. \quad (3c)$$

Here,  $\chi \equiv \xi + \frac{4}{3} \eta$  and  $t_d \equiv \tau/a$ .

We also need an equation of state to supplement Eqs. (3). We will only consider cases where  $P = P(\epsilon)$ , and investigate the sensitivity of the hydrodynamic evolution to the existence of a phase transition.

### III. SOURCE TERMS

We shall assume that heavy-ion collisions are made up of nucleon-nucleon collisions. Immediately after a nucleon-nucleon collision, the quanta produced undergo free streaming. At some proper time  $\tau_0$  later, they materialize, establish local thermal equilibrium, and thus begin the hydrodynamic era. Then, as shown in Ref. 3, the source terms can be built up as a direct summation of contributions from individual nucleon-nucleon collisions:

$$\begin{aligned} \Sigma^\mu &= \sum_{\text{collisions}} \sum_{i=\pi, N} \frac{m_i}{\mathcal{A}} \frac{x^\mu}{\tau_0^2} \frac{dN_i^{nn}}{dy} \delta(\tau - \tau_0), \\ \sigma_B &= \sum_{\text{collisions}} \frac{1}{\mathcal{A} \tau_0} \frac{dN_B^{nn}}{dy} \delta(\tau - \tau_0). \end{aligned}$$

Here,  $dN_B^{nn}/dy$  and  $dN_\pi^{nn}/dy$  are the baryon- and pion-number densities per unit rapidity produced in nucleon-nucleon collisions,  $m_\pi$  and  $m_N$  are the transverse pion and nucleon mass,  $\mathcal{A}$  is the transverse area of the colliding ions, and  $x^\mu = (t, z)$ . We have neglected the contributions to the source terms of heavier mesons and resonances. The inside-outside cascade (IOC) model says that most of  $\tau_0$  is due to formation time during which the produced quanta do not interact. Therefore, at high enough energies, a nucleon in the beam after a collision will materialize outside the volume of the colliding nuclide and will not make another collision with the target nucleons. The total number of primary nucleon-nucleon collisions is then equal to the total number of nucleon in each nucleus. Assuming uniform density distribution we can therefore replace the summation over all collisions by

$$n_0 \sinh y_0 \int \mathcal{A} dt$$

in the center-of-mass frame, with  $y_0$  being the rapidity and  $n_0$  the average proper density of each colliding ion. The source terms thus obtained are

$$\Sigma^0(y,s) = n_0 \sinh y_0 \sum_i \frac{m_i}{\tau_0} \frac{dN_i^{nn}}{dy}(y') \Theta(y,s), \quad (4a)$$

$$\sigma_B(y,s) = \frac{n_0 \sinh y_0}{\tau_0} \frac{dN_B^{nn}}{dy}(y') \times \frac{1}{(e^{2s} \sinh^2 y + 1)^{1/2}} \Theta(y,s), \quad (4b)$$

and

$$\Sigma^1(y,s) = \frac{e^s \sinh y}{(e^{2s} \sinh^2 y + 1)^{1/2}} \Sigma^0(y,s). \quad (4c)$$

Here,  $y' \equiv \text{arcsinh}[e^s \sinh(y)]$ , and  $\Theta$  is a step function representing the source region<sup>3</sup> (discussed below).

At the other extreme is the multiple-collision model<sup>15-17</sup> (MCM). In this model, most of  $\tau_0$  is due to a thermalization time during which the produced particles interact but have not yet established local thermal equilibrium. A nucleon in the beam can therefore make many collisions within the volume of the target nucleus, the probability of making a collision at transverse coordinate  $\mathbf{b}$  being  $P_B(\mathbf{b}) = T_B(\mathbf{b})\sigma_{\text{tot}}$ , where  $\sigma_{\text{tot}}$  is the total nucleon-nucleon cross section  $\approx 30$  mb, and  $T_B(\mathbf{b})$  is the normalized thickness function<sup>16</sup> for a nucleus

$$T_B(\mathbf{b}) = \int \rho(\mathbf{b}, z_B) dz_B$$

with  $\rho(\mathbf{b}, z_B)$  being the density (normalized to unity) at transverse and longitudinal coordinates  $\mathbf{b}$  and  $z_B$ , respectively, with the origin at the center of the nucleus. We will use a Wood-Saxon form for  $\rho$  with a diffuseness of 0.5 fm and radius  $R = 7$  fm for <sup>238</sup>U.

We formulate our version of the MCM in the target's rest frame where the beam ion is very much Lorentz contracted. It is therefore reasonable to make the approximation that all collisions between a nucleon in the target and the tube of beam nucleons at the same transverse coordinates occur at the same time and same place, which correspond to the overlap of the coordinates of the center of the projectile tube with those of the target nucleon. In the system of coordinates defined in Fig. 1(b),  $z_C = t_C \tanh y_0$ , where  $z_C, t_C$  are the space and time coordinates where the collisions occur. The average probability for a nucleon in a strip of the target of length  $\Delta z_C$  to make  $n$  collisions with the projectile nucleons is then

$$\Delta P^{(n)}(z_C) = \Delta z_C \binom{A}{n} \int d\mathbf{b} \rho(\mathbf{b}, z_C) [P_B(\mathbf{b})]^n \times [1 - P_B(\mathbf{b})]^{A-n}, \quad (8)$$

where  $A$  is the total number of nucleons in each colliding nucleus.

From the observation that a nucleon is scattered into the entire range of possible Feynman  $x$  with approximately uniform distribution, and assuming Feynman scaling,<sup>18</sup> Wong<sup>17</sup> obtained the rapidity distribution of target baryons after  $n$  collisions:

$$D_t^{(n)}(y) = \frac{e^{y_0-y}}{2 \sinh y_0} \frac{1}{(n-1)!} \times \left[ \ln \left[ \frac{2 \sinh y_0}{e^{y_0-y} - e^{-y_0}} \right] \right]^{(n-1)} \times \theta(2y_0 - y) \theta(y), \quad n \geq 1, \quad (5)$$

$$D_t^{(0)}(y) = \delta(y).$$

We can then sum  $D_t^{(n)}(y)$  weighted by  $\Delta P^{(n)}$  over  $n$  to obtain the contributions of the slab at  $z_C$  to the target net baryon rapidity density:

$$\Delta \frac{dN_B^{\text{slab}}}{dy} = A \sum_{n=0}^A D_t^{(n)}(y') \Delta P^{(n)}(z_C). \quad (6)$$

Equation (6) is then summed over all slabs in the target to get the contributions of the target to the baryon-number current source term

$$\sigma_B^t = \sum_{\text{slabs}} \Delta \frac{dN_B^{\text{slab}}}{dy} \frac{1}{\tau_0 \mathcal{A}(z_C)} \delta(\tau - \tau_0),$$

with  $\mathcal{A}(z_C) = \pi(2R |z_C| - z_C^2)$  being the transverse area of the target nucleus at  $z_C$ . We can now go back to the center-of-mass frame and add together the contributions from the target and the projectile nucleus, the latter being just the mirror image of the former with respect to  $y=0$ :

$$\sigma_B(y,s) = \frac{\sinh y_0}{\tau_0} \sum_{n=0}^A D^{(n)}(y') G^{(n)}(z_C = at_0) \times \frac{\Theta(y,s)}{(e^{2s} \sinh^2 y + 1)^{1/2}}, \quad (7a)$$

where

$$G^{(n)}(z_C) = \binom{A}{n} \int d\mathbf{b} \rho(\mathbf{b}) [T_B(\mathbf{b})\sigma_{\text{tot}}]^n \times [1 - T_B(\mathbf{b})\sigma_{\text{tot}}]^{A-n} \frac{A}{\mathcal{A}(z_C)}, \quad (8)$$

with

$$t_0 = \tau_0 \cosh y_0 [e^s \cosh y - (e^{2s} \sinh^2 y + 1)^{1/2}]$$

the time at which collisions occur (in the rest frame of the target, but expressed in center-of-mass  $y$ ), and

$$D^{(n)}(y) = \frac{\theta(y_0+y)\theta(y_0-y)}{2 \sinh y_0 (n-1)!} \left\{ e^y \left[ \ln \left[ \frac{2 \sinh y_0}{e^y - e^{-y_0}} \right] \right]^{(n-1)} + e^{-y} \left[ \ln \left[ \frac{2 \sinh y_0}{e^{-y} - e^{-y_0}} \right] \right]^{(n-1)} \right\}, \quad n \geq 1,$$

$$D^{(0)}(y) = \frac{1}{\sqrt{2\pi\sigma_x}} \left[ \exp \left[ \frac{-[\exp(-y+y_0)-1]^2}{2\sigma_x^2} \right] \exp(y-y_0) + \exp \left[ \frac{-[\exp(-y-y_0)-1]^2}{2\sigma_x^2} \right] \exp(-y-y_0) \right].$$

Note that we have smeared out  $D^{(0)}(y)$  with  $\sigma_x \approx 0.1$  because of Fermi motion, which has only a small effect on  $n \neq 0$  terms. If uniform density distribution in each of the colliding  $^{238}\text{U}$  ions is assumed, this model predicts that a nucleon in either ions will suffer 3.5 collisions in average.

The treatment of the produced pions is only slightly different. In this case, we have to sum up contributions from all collisions:

$$\Delta \frac{dN_{\pi}^{\text{slab}}}{dy} = \sum_{n=1}^A G_{\text{in}}^{(n)}(z_C) \Delta z_C \rho_{\pi}^{(n)},$$

with

$$\rho_{\pi}^{(n)} \equiv \sum_{j=1}^n \frac{dN_{\pi}^{nn}}{dy}(\sqrt{s_j}, y').$$

Here  $\sqrt{s_j} = m_N \cosh(y_0 - j + 1)$  is the center-of-mass energy of a nucleon just before its  $j$ th collision, and the elastic term ( $n=0$ ) is excluded. Note that Eq. (5) implies that a nucleon in the beam losses in average one unit of rapidity per collision<sup>17</sup> (except for the first one, which just smears out the rapidity distribution), and we have downgraded its energy accordingly.  $G_{\text{in}}^{(n)}$  is the same as  $G^{(n)}$  except that the inelastic cross section  $\sigma_{\text{in}}$  should be used in place of  $\sigma_{\text{tot}}$  in Eq. (8). We thus have, in the center-of-mass frame,

$$\begin{aligned} \Sigma^0(y, s) = \frac{\sinh y_0}{\tau_0} & \left[ m_{\pi} \sum_{n=1}^A G_{\text{in}}^{(n)}(at_0) \rho_{\pi}^{(n)}(\sqrt{s_j}, y') \right. \\ & \left. + m_N \sum_{n=0}^A D^{(n)}(y') G^{(n)}(at_0) \right] \\ & \times \Theta(y, s) \end{aligned} \quad (7b)$$

and

$$\Sigma^1(y, s) = \frac{e^s \sinh y}{(e^{2s} \sinh^2 y + 1)^{1/2}} \Sigma^0(y, s). \quad (7c)$$

The boundaries of the source region for the IOC are given in Ref. 3, and we just summarize their results here. The hydrodynamic source terms should be turned off (1) before the products of the first collisions and after those from the last collisions have thermalized,

$$s \leq 0,$$

or

$$s \geq \ln \left\{ \frac{d_t}{\tau_0} \cosh y + \left[ \left( \frac{d_t}{\tau_0} \right)^2 \sinh^2 y + 1 \right]^{1/2} \right\},$$

with  $d_t \equiv 2R/\sinh y_0$  being the time it takes the two colliding ions to pass through each other, and (2) after all the momentum of a nucleon is lost:

$$|y| \leq \text{arcsinh}(e^{-s} \sinh y_0).$$

As formulated above, the MCM shares the same source boundaries as in the IOC.

For the numerical calculations presented below, we assume central collisions of  $^{238}\text{U}$  ions with  $R=7$  fm and  $n_0=0.166$  fm<sup>-3</sup>. We will use the following parametrization of experimental nucleon-nucleon data:<sup>3,19</sup>

$$\begin{aligned} \frac{dN_{\pi}^{nn}}{dy}(y, \sqrt{s_j}) = & (0.83 \ln \sqrt{s_j} - 0.39) \\ & \times \left[ 1 - \frac{m_{\pi}}{\sqrt{s_j}} \cosh y \right]^3, \end{aligned} \quad (9a)$$

$$\frac{dN_B^{nn}}{dy}(y) = \frac{\cosh y}{\sinh y_0}. \quad (9b)$$

We will also take the transverse pion mass  $m_{\pi}=0.5$  GeV and  $m_N=1$  GeV.

#### IV. NUMERICAL METHOD AND RESULTS

The system of Eqs. (3a)–(3c) with the source terms given by (4a)–(4c) for IOC and (7a)–(7c) for MCM using (9a) and (9b) can be solved by straightforward discretization of the  $(\hat{u}, \hat{v})$  plane, which is related to the  $(y, s)$  plane through Eq. (2). The initial conditions, i.e.,  $n_B=0$ ,  $\epsilon=P=0$ , and  $\theta=y$  are implemented on the  $s=0$  axis, which coincides with  $\hat{v}=0$ . The finite difference equation corresponding to (3a) is then used to evolve  $\epsilon$  in the  $\hat{v}$  direction, while that corresponding to (3b) evolves  $\theta$ . We use a simple forward scheme to calculate finite differences in the  $\hat{v}$  direction while centering all finite differences in the  $\hat{u}$  direction. These difference equations are given in the Appendix. We first solve (3a) and (3b) for  $\epsilon$  and  $\theta$ , and then feed  $\theta$  into (3c) to obtain  $n_B$  at each iteration in  $\hat{v}$ . Typical step size used is  $\Delta u=0.02$  and  $\Delta v=0.002$ . At beam energy of 14 GeV/nucleon, assuming  $\tau_0=1$  fm, pion plateau height of 2.4, and with the viscosity turned off, our results agree with those in Ref. 3.

Samples of the results of our calculations are shown in Figs. 2–10. We now discuss the dependence of the hydrodynamic evolution on  $\tau_0$ , the viscosity, the equation of state, beam energy, and the model of source terms.

(i) *Dependence on  $\tau_0$ .* First we consider the effects of changing  $\tau_0$ . As shown in Figs. 2(a), 3(a), and 4, the max-

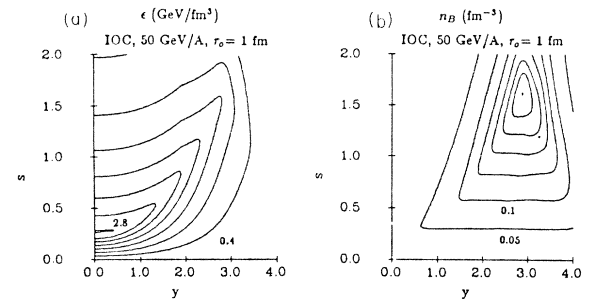


FIG. 2. Contour plots for (a) energy density in GeV/fm<sup>3</sup>, and (b) net-baryon-number density in fm<sup>-3</sup> for a central collision of  $^{238}\text{U}$  ions at 50 GeV/nucleon each. An inside-outside cascade is assumed, with  $\tau_0=1$  fm. The coefficient of shear viscosity  $\eta$  is taken from Ref. 13, assuming a relaxation time of 1 fm, and the coefficient of bulk viscosity  $\xi$  is ignored here. The bag-model equation of state is used [Eq. (10) in text]. Contours are drawn in steps of (a) 0.4 GeV/fm<sup>3</sup>, from 0.4 to 2.8 GeV/fm<sup>3</sup>, and (b) 0.05 fm<sup>-3</sup>, from 0.05 to 0.35 fm<sup>-3</sup>.

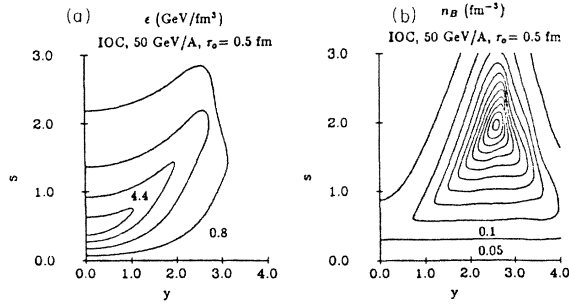


FIG. 3. Same as Fig. 2 except that  $\tau_0=0.5$  fm. Contours are drawn in steps of (a) 1.2 GeV/fm<sup>3</sup>, from 0.8 to 4.4 GeV/fm<sup>3</sup>, and (b) 0.05 fm<sup>-3</sup>, from 0.05 to 0.55 fm<sup>-3</sup>.

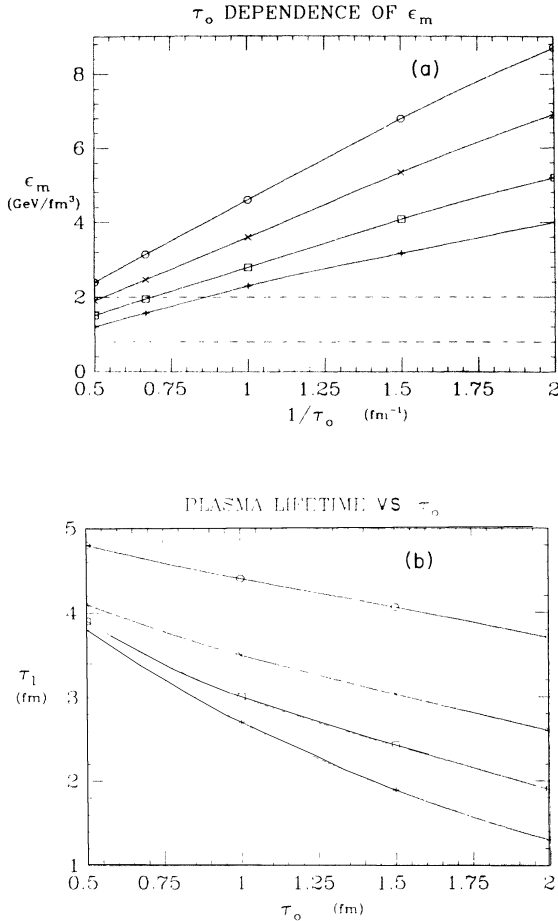


FIG. 4.  $\tau_0$  dependence of (a) maximum energy density  $\epsilon_m$  and (b) plasma lifetime  $\tau_l$ . Collisions of 30 and 100 GeV/nucleon (pluses with holes and crosses, respectively) are shown for the inside-outside cascade (IOC) model, and 50 GeV/nucleon for both IOC (squares) and the multiple-collision model (MCM, circles). In (a) the dashed lines correspond to the boundaries of the mixed phase for the bag-model equation of state used. In (b) the plasma lifetime is defined as the proper-time duration for which the energy density at  $z=0$  is higher than 0.8 GeV/fm<sup>3</sup>. The solid lines are drawn to guide the eyes.

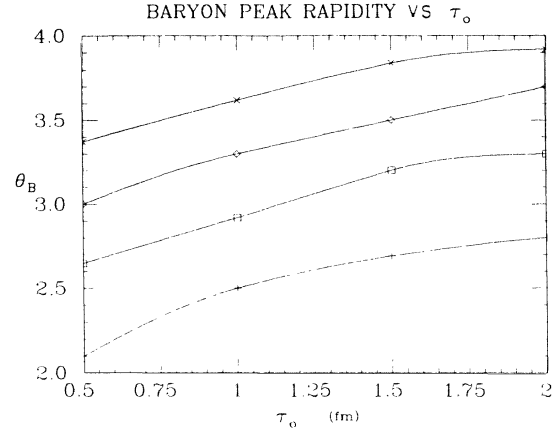


FIG. 5.  $\tau_0$  dependence of the baryon peak rapidity in IOC, shown for  $E=30$  (pluses), 50 (squares), 70 (diamonds), and 100 (crosses) GeV/nucleon. The solid lines are drawn to guide the eyes.

imum energy density reached  $\epsilon_m$  is strongly affected by  $\tau_0$ . Bjorken's estimation for the  $\tau_0$  dependence of the initial energy density,  $\epsilon_m \sim 1/\tau_0$  is slightly modified. As a result of the difference in energy density, the proper lifetime of the plasma  $\tau_l$  also changes as a function of  $\tau_0$ , although not as fast as  $\epsilon_m$ . Assuming IOC, if  $\tau_0$  is as long as 2 fm, this study shows that even at 100 GeV/nucleon, the energy density created in a heavy-ion collision will not be high enough to reach the pure quark-gluon phase ( $\epsilon \geq 2$  GeV/fm<sup>3</sup>), while if  $\tau_0$  is only 0.5 fm, 30 GeV/nucleon is sufficient. Both  $\epsilon_m$  and  $\tau_l$  given here are lower than earlier estimates; this reflects the diluting effect of hydrodynamics when the source term is effective for finite duration. Figures 2(b), 3(b), and 5 also shows that the degradation of the rapidity of the outgoing fragments in IOC increases as  $\tau_0$  decreases. This can be understood in the following way: the baryons lose some of their momenta when thermalized with the slower moving plasma; if  $\tau_0$  is smaller, the baryons materialize at smaller  $y$  in average, and thus they suffer more rapidity degradation. This additional rapidity loss of the fragmentation region in heavy-ion collisions when compared to that of

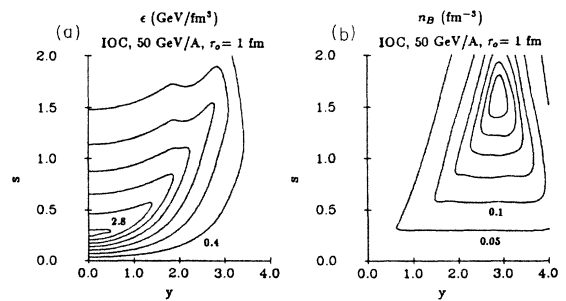


FIG. 6. Same as Fig. 2 except that  $\xi$  is equal to  $\eta$  when the energy density falls to below 2 GeV/fm<sup>3</sup>. Contours are drawn in steps of (a) 0.4 GeV/fm<sup>3</sup>, from 0.4 to 2.8 GeV/fm<sup>3</sup>, and (b) 0.05 fm<sup>-3</sup>, from 0.05 to 0.3 fm<sup>-3</sup>.

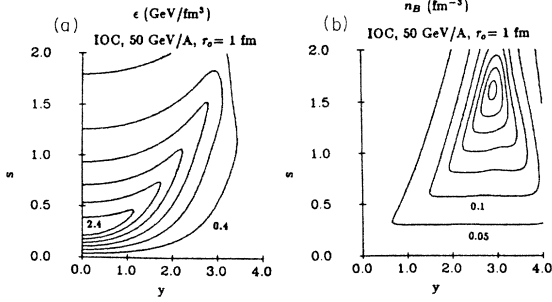


FIG. 7. Same as Fig. 2 except that the ideal gas equation of state with no phase transition,  $P = \epsilon/3$  is used. Contours are drawn in steps of (a) 0.4 GeV/fm<sup>3</sup>, from 0.4 to 2.4 GeV/fm<sup>3</sup>, and (b) 0.05 fm<sup>-3</sup>, from 0.05 to 0.35 fm<sup>-3</sup>.

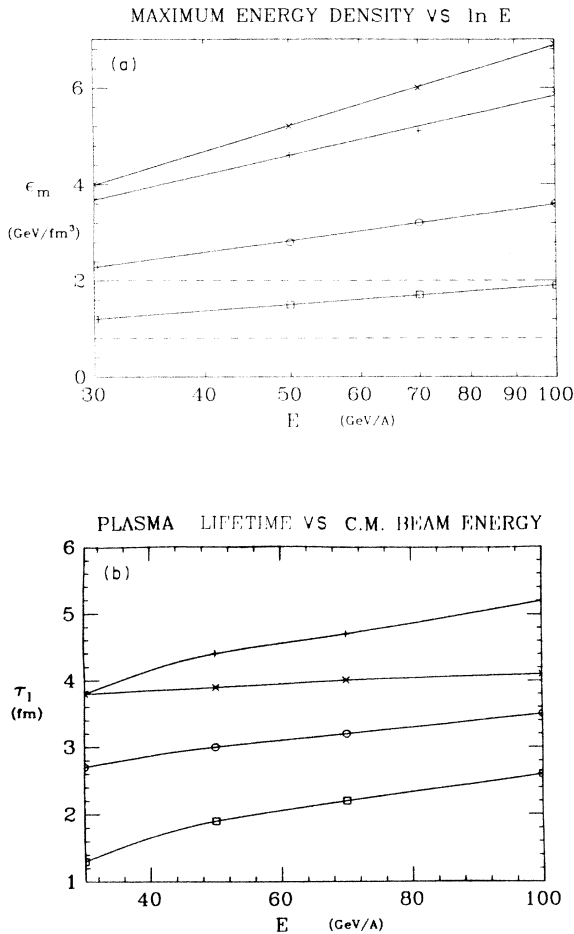


FIG. 8. Beam energy (in center-of-mass frame) dependence of (a) maximum energy density, and (b) plasma lifetime.  $\tau_0 = 0.5$  and 2 fm are shown for IOG (crosses and squares), and  $\tau_0 = 1$  fm is shown for both IOG (circles) and MCM (pluses). In (a) the dashed lines correspond to the boundaries of the mixed phase for the bag-model equation of state used. The solid lines are fit to  $\epsilon_m = c \ln E + d$ ,  $c$  and  $d$  being constants. In (b) the solid lines are drawn to guide the eyes.

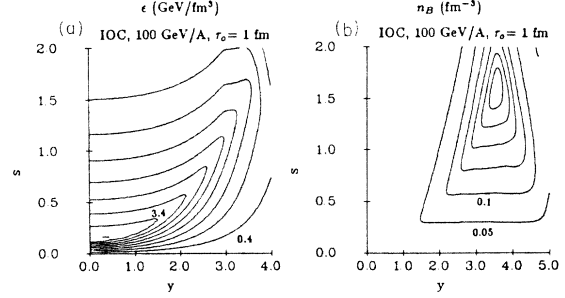


FIG. 9. Same as Fig. 2 except that the collision energy is 100 GeV/nucleon for each ion. Contours are drawn in steps of (a) 0.4 GeV/fm<sup>3</sup>, from 0.4 to 3.8 GeV/fm<sup>3</sup>, and (b) 0.05 fm<sup>-3</sup>, from 0.05 to 0.3 fm<sup>-3</sup>.

nucleon-nucleon data, can be regarded as a signature of collective effects. Unfortunately, this effect is swamped by the much larger rapidity downshifting inherent in MCM.

Another feature associated with a smaller  $\tau_0$  is the increase in sharpness of the baryon peak. This is obviously a result of the smaller space-time region in which the baryons materialize if  $\tau_0$  is small.

One last remark on  $\tau_0$ : scaling is violated more severely for smaller  $\tau_0$ . Scaling is exact in the limit of an infinitely long plasma tube. The smaller  $\tau_0$  is, the shorter the plasma tube is, and hence the larger deviations from scaling. This, together with the opening up of the low-baryon-number region, makes Bjorken's scaling picture a better approximation for large  $\tau_0$ .

(ii) *Dependence on viscosity.* The coefficients of viscosity of the quark-gluon plasma have been studied with a relaxation-time method<sup>13</sup> and with QCD phenomenology.<sup>6</sup> The results of these two calculations cannot be compared directly with each other because of the unknown temperature dependence of the relaxation time  $\tau_r$ . Near the phase transition temperature, the coefficients of viscosity may be greatly suppressed due to large nonperturbative effects and, as a result, there are large uncertainties in the estimation of the transport coefficients. We shall use the results from Ref. 13 with a relaxation time of 1 fm, which gives

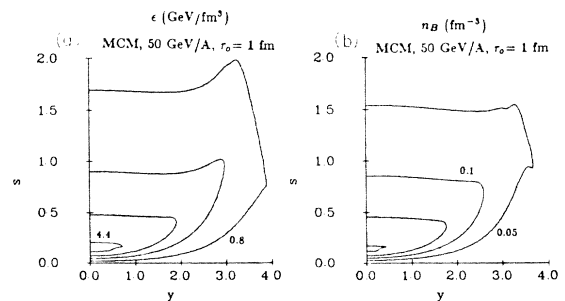


FIG. 10. Same as Fig. 2 except that the MCM is assumed. Contours are drawn in steps of (a) 1.2 GeV/fm<sup>3</sup>, from 0.8 to 4.4 GeV/fm<sup>3</sup>, and (b) 0.05 fm<sup>-3</sup>, from 0.05 to 0.2 fm<sup>-3</sup>.

values of  $\eta \approx 1.1 \text{ GeV fm}^{-2}$  at  $T=300 \text{ MeV}$ , decreasing to  $\eta \approx 0.2 \text{ GeV fm}^{-2}$  at  $T=200 \text{ MeV}$ . Assuming a characteristic length of  $10 \text{ fm}$ , the classical Reynold number of the system is typically about 40.

We have done calculations using coefficients from both Refs. 6 and 13, finding no significant difference in the results. We have also tried two values of  $\tau_r$  (0.5, 1.0 fm), again finding that the results are little affected. The coefficient of bulk viscosity  $\xi$  is very small in the plasma phase, but may become comparable to  $\eta$  in the mixed and the hadronic phase.<sup>6</sup> We show in Fig. 6 results of our calculations assuming  $\xi=\eta$  for  $\epsilon \leq 2 \text{ GeV/fm}^3$ . Comparing with Fig. 2, we find that the hydrodynamic behavior for  $\xi=0$  and for  $\xi=\eta$  does not differ very much. The only effect of the viscosity we observe is a slight increase of  $\tau_l$  ( $\approx 10\%$  for the case shown in Figs. 2 and 6) and  $\epsilon_m$  (just a few percent) if larger coefficients of viscosity are used. This is simply explained in terms of a slower flow rate when the fluid is more viscous. The effects of the viscosity on the lifetime of the plasma as measured in the center-of-mass frame will be even smaller due to the fact that slower plasma flow means less time dilation, which compensates the small gain in proper lifetime. Overall, viscosity does not seem to be an important ingredient of the (one-dimensional) hydrodynamics of high-energy heavy-ion collisions.

(iii) *Equation of state.* Lattice gauge calculations<sup>20</sup> show that a pure gluon plasma behaves like an ideal Stefan-Boltzmann gas for temperatures not too close to the critical point of the deconfinement transition. We therefore use two extreme equations of state in this calculation: that of an ideal relativistic gas (1) with no phase transition,  $P = \epsilon/3$ , and (2) with a first-order phase transition motivated by the bag model:<sup>21</sup>

$$P = \begin{cases} \epsilon/3, & 0 \leq \epsilon \leq \epsilon_l, \\ \epsilon_l/3, & \epsilon_l \leq \epsilon \leq \epsilon_u, \\ (\epsilon - \epsilon_u + \epsilon_l)/3, & \epsilon \geq \epsilon_u. \end{cases} \quad (10)$$

Here,  $\epsilon_l$  and  $\epsilon_u$  are the lower and upper boundaries of the mixed phase, chosen to be  $0.8$  and  $2 \text{ GeV fm}^{-3}$ , respectively, for the results presented here. Changing the numerical values of  $\epsilon_l$  and  $\epsilon_u$ , or using a pion gas equation of state with finite pion mass for the hadronic phase does not change the results significantly.

A comparison of the results for the two equations of state used shows that while the lifetime of the plasma is longer for a bag-model equation of state (by about 15% for the case shown in Figs. 2 and 7), most other features of the hydrodynamic flow are insensitive to the equation of state (cf. Figs. 2 and 7). This is in accord with the findings of Ref. 22 for Landau hydrodynamics. The small difference in the plasma lifetime can be explained by the fact that at the mixed-phase region the speed of sound becomes zero, and therefore the expansion is slower than if there were no phase transitions. We should remark that we have treated the first-order phase transition within the framework of mean-field theory (and for nu-

merical reason, we have also introduced a small smearing of the equation of state so that the slope is not discontinuous at  $\epsilon_l$  and  $\epsilon_u$ ). It is quite possible that we miss some drastic phenomena<sup>23</sup> due to the phase transition.

(iv) *Dependence on beam energies.* Since the pion plateau height in nucleon-nucleon collisions increases as  $\ln E$  for increasing collision energy  $E$  up to  $100 \text{ GeV/nucleon}$  (Ref. 17), we expect that the maximum energy density achieved in heavy-ion collisions also goes as  $\epsilon_m = c \ln E + d$ ,  $c$  and  $d$  being constants. In Fig. 8(a) we show this fit to our results for energies up to  $100 \text{ GeV/nucleon}$ . In both models of the source, the lifetime of the plasma, however, does not increase significantly as we raise  $E$  from  $30$  to  $100 \text{ GeV/nucleon}$  [see Fig. 8(b)]. While collisions with higher energies create plasma with higher energy density, the speed of the hydrodynamic flow is also higher. The duration it takes the plasma to cool down to the critical temperature is thus quite insensitive to the collision energy (cf. Figs. 2 and 9). Another feature associated with increasing  $E$  is the opening up of the low-baryon-number region in the IOC. The MCM, on the other hand, does not give such a gap in the range of energies considered here.

(v) *Source terms.* The two models of source terms we use here are very different, and indeed they lead to drastically different results (cf. Figs. 2 and 10). As expected, the baryons in the MCM dissipate more energies and momenta than in IOC. Therefore, in the MCM the maximum energy density is higher, while the baryon rapidity is lower than in IOC. As a consequent, the plasma lifetime in MCM is longer than that in IOC. Another obvious signature of the MCM as compared to the IOC is the large rapidity smearing of the baryon peaks. In fact, for the MCM, our calculations show that the net baryon number is distributed almost uniformly in the final states.

## V. CONCLUSION

From the calculations presented above, we can draw the following conclusions.

(1) Viscosity is not essential for a qualitative understanding of the hydrodynamics of ultrarelativistic heavy-ion collision.

(2) Neither is the equation of state.

(3) The hadronization time  $\tau_0$  is an important parameter. Before pinning down this parameter more accurately, we cannot even say at what beam energies quark-gluon plasma should be produced. In the IOC, the rapidity loss of the baryon peaks may provide a clue to the magnitude of  $\tau_0$  (smaller rapidity loss for larger  $\tau_0$ ).

(4) The chances for creating a quark-gluon plasma ( $\epsilon_m \geq 2 \text{ GeV/fm}^3$ ) increase only as the logarithm of the beam energies.

(5) Results for the MCM and the IOC differ so much that one cannot with confidence say that either approximates reality well. But we do expect that reality lies somewhere between these two models.

It is clear, then, that a better understanding of  $\tau_0$  and the source terms is urgently needed for further theoretical investigation of the physics of ultrarelativistic heavy-ion collisions.

## ACKNOWLEDGMENTS

The author thanks Dr. S. E. Koonin for many helpful discussions and encouragement. This work was supported by National Science Foundation Grants Nos. PHY85-05682 and PHY82-07332.

## APPENDIX

To solve Eqs. (3), we first locate the  $(u, v)$  grid points on the  $(y, s)$  plane by discretizing Eq. (2):

$$\frac{y_i^{j+1} - y_i^j}{s_i^{j+1} - s_i^j} = \tanh(\theta_i^j - y_i^j), \quad (\text{A1})$$

and

$$\frac{s_i^{j+1} - s_{i-1}^{j+1}}{y_i^{j+1} - y_{i-1}^{j+1}} + \frac{s_{i-1}^{j+1} - s_{i-2}^{j+1}}{y_{i-1}^{j+1} - y_{i-2}^{j+1}} = 2 \tanh(\theta_{i-1}^{j+1} - y_{i-1}^{j+1}), \quad (\text{A2})$$

where the lower (upper) index labels positions on  $\hat{u}$  ( $\hat{v}$ ). These equations represent the curves along  $\hat{v}$ ,  $\hat{u}$  directions, and their intersections are the grid points. Examples of these curves on the  $y$ - $s$  plane are shown in Fig. 11. Notice that the curves in the  $\hat{u}$  direction start out from the  $y=0$  axis initially perpendicular to the  $s$  axis. The viscosity slows down the flow resulting in a slight diving of the  $u$  curves towards the  $y$  axis, but the huge pressure gradient

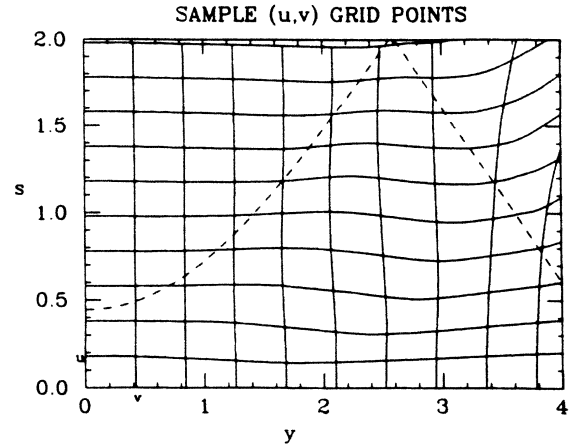


FIG. 11. Sample  $(u, v)$  grid points on the  $y$ - $s$  plane. The dashed lines mark the boundaries of the source region.

at the end of the source region accelerates the plasma causing the curves to bend up after passing through the source region. If perfect scaling holds, these curves just form rectangular grids.

We then solve the difference equations corresponding to Eqs. (3) on the grid points generated with Eq. (A1) and Eq. (A2):

$$\epsilon_i^{j+1} = \epsilon_i^j + \Delta v_i^j \left[ \left( \frac{\chi_i^j}{(t_d)_i^j} \theta_i^{j+1} - (\epsilon_i^j + P_i^j) \right) \theta_i^{j+1} + (t_d)_i^j (S_1)_i^j \right], \quad (\text{A3a})$$

$$\theta_i^{j+1} = \theta_i^j + \left[ (\epsilon_i^j + P_i^j) - \frac{\chi_i^j}{(t_d)_i^j} \right]^{-1} \Delta v_i^j \left[ \frac{1}{(t_d)_i^j} \{ \chi_i^j [(a_1)_i^j \theta_i^{j+1} - (a_2)_i^j \theta_i^j + \chi_i^j \theta_i^{j+1} + \chi_i^{j+1}] + (t_d)_i^j (S_2)_i^j - P_i^{j+1} \right], \quad (\text{A3b})$$

and

$$(n_B)_i^{j+1} = (n_B)_i^j + \Delta v_i^j [(t_d)_i^j \sigma_{Bj} - (n_B)_i^j \theta_i^{j+1}]. \quad (\text{A3c})$$

We have used the following notations:

$$A_i^{j,j} = \frac{A_{i+1}^j - A_{i-1}^j}{2\Delta u_i^j},$$

$$A_i^{j,j} = \frac{1}{2} \left[ \frac{A_{i+1}^j - A_i^j}{\Delta u_i^j} + \frac{A_i^j - A_{i-1}^j}{\Delta u_{i-1}^j} \right],$$

and

$$a_1 \equiv \frac{2\alpha\beta}{a^2}, \quad a_2 \equiv \frac{\alpha}{a} \left[ 2 \frac{\beta^2}{a^2} + 1 \right].$$

For stability reason, in the second terms of both Eq. (3a) and Eq. (3c),  $\partial_u \theta$  is evaluated at  $v = (j+1)\Delta v$ , while  $(\epsilon + P)$  in (3a) and  $n_B$  in (3c) are calculated at  $v = j\Delta v$ . Without the viscosity term, this scheme is stable as long as the rapidity gradient does not become negative. We expect that the viscosity term will improve the numerical stability even if a shock front is developed.

<sup>1</sup>For a review, see B. Müller, *The Physics of the Quark-Gluon Plasma* (Lecture Notes in Physics, Vol. 225) (Springer, Heidelberg, 1985); E. V. Shuryak, *Phys. Rep.* **61**, 71 (1980). See, also, *Proceedings of the First Workshop on Ultra-Relativistic Nuclear Collisions, Berkeley, California, 1979* (Lawrence Berkeley Laboratory, Berkeley, 1979); *Statistical Mechanics of*

*Quarks and Hadrons*, edited by H. Satz (North-Holland, Amsterdam, 1981); *Quark Matter Formation and Heavy Ion Collisions*, edited by M. Jacob and H. Satz (World Scientific, Singapore, 1982); *Quark Matter '83*, proceedings of the Third International Conference on Ultrarelativistic Nucleon-Nucleus Collisions, Brookhaven National Laboratory, 1983,

- edited by T. W. Ludlam and H. E. Wegner [Nucl. Phys. **A418** (1984)]; *Quark Matter '84*, proceedings of the Fourth International Conference on Ultrarelativistic Nucleus-Nucleus, edited by K. Kajantie (Lecture Notes in Physics, Vol. 221) (Springer, New York, 1985).
- <sup>2</sup>J. D. Bjorken, Phys. Rev. D **27**, 140 (1983); G. Baym *et al.*, Nucl. Phys. **A407**, 541 (1983).
- <sup>3</sup>K. Kajantie, R. Raitio, and P. V. Ruuskanen, Nucl. Phys. **B222**, 152 (1983); K. Kajantie and L. McLerran, *ibid.* **B214**, 261 (1983); Phys. Lett. **119B**, 203 (1982); K. Kajantie and R. Raitio, *ibid.* **121B**, 415 (1983).
- <sup>4</sup>H. W. Barz, B. Kämpfer, L. P. Csernai, and B. Lukács, Phys. Lett. **143B**, 334 (1984); H. W. Barz, B. Kämpfer, L. P. Csernai, and B. Lukács, Phys. Rev. C **31**, 268 (1985).
- <sup>5</sup>M. Gyulassy and T. Matsui, Phys. Rev. D **29**, 419 (1984).
- <sup>6</sup>P. Danielewicz and M. Gyulassy, Phys. Rev. D **31**, 53 (1985).
- <sup>7</sup>M.-C. Chu, Phys. Rev. C **31**, 1739 (1985).
- <sup>8</sup>R. B. Clare and D. Strottman, Los Alamos National Laboratory report, 1985 (unpublished).
- <sup>9</sup>W. Busza and A. S. Goldhaber, Phys. Lett. **139B**, 235 (1984); W. Busza, Nucl. Phys. **A418**, 635c (1984).
- <sup>10</sup>J. D. Bjorken, in *Lecture Notes on Current-Induced Reactions*, edited by J. Körner, G. Kramer, and D. Schildknecht (Springer, New York, 1975); J. Kogut and L. Susskind, Phys. Rev. D **10**, 732 (1974).
- <sup>11</sup>L. D. Landau and E. M. Lifshitz, *Fluid Mechanics* (Pergamon, London, 1959).
- <sup>12</sup>B. Banerjee, N. K. Glendenning, and T. Matsui, Phys. Lett. **127B**, 453 (1983).
- <sup>13</sup>Sean Gavin, Nucl. Phys. **A435**, 826 (1985).
- <sup>14</sup>R. Courant and K. Friedrichs, *Supersonic Flow and Shock Waves* (Springer, New York, 1976).
- <sup>15</sup>R. J. Glauber, in *Lectures in Theoretical Physics*, edited by W. E. Brittin and L. G. Dunham (Interscience, New York, 1959), Vol. 1, p. 315; R. Blenkenbecler *et al.*, Phys. Lett. **107B**, 106 (1981).
- <sup>16</sup>C. Y. Wong, Phys. Rev. D **30**, 972 (1984); **32**, 94 (1985); J. Kapusta, Phys. Rev. C **27**, 2037 (1983).
- <sup>17</sup>C. Y. Wong, Phys. Rev. Lett. **52**, 1393 (1984).
- <sup>18</sup>F. E. Taylor *et al.*, Phys. Rev. D **14**, 1217 (1976).
- <sup>19</sup>W. Thomé *et al.*, Nucl. Phys. **B129**, 365 (1977); K. Alpgård *et al.*, Phys. Lett. **107B**, 315 (1981).
- <sup>20</sup>J. Engels *et al.*, Nucl. Phys. **B205**, 545 (1982); I. Montvay and E. Pietarinen, Phys. Lett. **110B**, 148 (1982).
- <sup>21</sup>A. Chodos, R. L. Jaffe, C. B. Thorn, and V. Weisskopf, Phys. Rev. D **9**, 3471 (1974); A. Chodos, R. L. Jaffe, K. Johnson, and C. B. Thorn, *ibid.* **10**, 2599 (1974); T. DeGrand, R. L. Jaffe, K. Johnson, and J. Kiskis, *ibid.* **12**, 2060 (1975).
- <sup>22</sup>K. Wehrberger and R. M. Weiner, Phys. Rev. D **31**, 222 (1985).
- <sup>23</sup>M. Gyulassy, K. Kajantie, H. Kurki-Suonio, and L. McLerran, Nucl. Phys. **B237**, 477 (1984).